



DCE-MRI Quantitative Parameters as Predictors of Treatment Response in Patients With Locally Advanced Cervical Squamous Cell Carcinoma Underwent CCRT

OPEN ACCESS

Edited by:

Fu Wang,
Xidian University, China

Reviewed by:

Yuming Jiang,
Stanford University, United States
Guolin Ma,
China-Japan Friendship Hospital,
China

*Correspondence:

Yi Huan
huanyi3000@163.com
Min-Wen Zheng
zhengmw2007@163.com

[†]These authors have contributed
equally to this work

Specialty section:

This article was submitted to
Cancer Imaging and
Image-directed Interventions,
a section of the journal
Frontiers in Oncology

Received: 21 July 2020

Accepted: 22 September 2020

Published: 29 October 2020

Citation:

Liu B, Sun Z, Ma W-L, Ren J,
Zhang G-W, Wei M-Q, Hou W-H,
Hou B-X, Wei L-C, Huan Y and
Zheng M-W (2020) DCE-MRI
Quantitative Parameters as
Predictors of Treatment Response
in Patients With Locally Advanced
Cervical Squamous Cell
Carcinoma Underwent CCRT.
Front. Oncol. 10:585738.
doi: 10.3389/fonc.2020.585738

Bing Liu^{1†}, Zhen Sun^{2†}, Wan-Ling Ma³, Jing Ren¹, Guang-Wen Zhang¹, Meng-Qi Wei¹, Wei-Huan Hou¹, Bing-Xin Hou⁴, Li-Chun Wei⁴, Yi Huan^{1*} and Min-Wen Zheng^{1*}

¹ Department of Radiology, Xijing Hospital, Fourth Military Medical University, Xi'an, China, ² Department of Orthopedic, Xijing Hospital, Fourth Military Medical University, Xi'an, China, ³ Department of Radiology, Longgang District People's Hospital, Shenzhen, China, ⁴ Department of Radiation Oncology, Xijing Hospital, Fourth Military Medical University, Xi'an, China

Purpose: To evaluate the predictive value of dynamic contrast-enhanced magnetic resonance imaging (DCE-MRI) quantitative parameters in treatment response to concurrent chemoradiotherapy (CCRT) for locally advanced cervical squamous cell carcinoma (LACSC).

Methods and materials: LACSC patients underwent CCRT had DCE-MRI before (e0) and after 3 days of treatment (e3). Extended Tofts Linear model with a user arterial input function was adopted to generate quantitative measurements. Endothelial transfer constant (K^{trans}), reflux rate (K_{ep}), fractional extravascular extracellular space volume (V_e), and fractional plasma volume (V_p) were calculated, and percentage changes ΔK^{trans} , ΔK_{ep} , ΔV_e , and ΔV_p were computed. The correlations of these measurements with the tumor regression rate were analyzed. The predictive value of these parameters on treatment outcome was generated by the receiver operating characteristic (ROC) curve. Univariate and multivariate logistic regression analyses were conducted to find the independent variables.

Results: $K^{trans-e0}$, K_{ep-e0} , ΔK^{trans} , and ΔV_e were positively correlated with the tumor regression rate. Mean values of $K^{trans-e0}$, $K^{trans-e3}$, ΔK^{trans} , and ΔV_e were higher in the non-residual tumor group than residual tumor group and were independent prognostic factors for predicting residual tumor occurrence. $K^{trans-e3}$ showed the highest area under the curve (AUC) for treatment response prediction.

Conclusions: Quantitative parameters at e0 and e3 from DCE-MRI could be used as potential indicators for predicting treatment response of LACSC.

Keywords: cervical cancer, dynamic contrast-enhanced magnetic resonance imaging, concurrent chemoradiotherapy, Tofts DCE-MRI model, treatment response

INTRODUCTION

Cervical cancer is the fourth leading cause of cancer death in women worldwide (1). Concurrent chemoradiotherapy (CCRT) is the primary choice for locally advanced cervical cancer patients, with significant benefits even for the advanced-stage disease (2). Although the alternative or novel treatment modalities could potentially improve treatment outcomes further, there is concern regarding treatment toxicity and complications in survivors (3). Moreover, even with the same clinical stage and pathological subtype, the prognosis differs among patients, which indicates tumor heterogeneity and distinct radio-sensitivity. Techniques providing composite prognostic information than current clinical prognostic factors like stage, grade, histology, and patients comorbidities would allow individualization of treatment (4). Techniques that reflect biological changes during the complex process of chemoradiotherapy are of great importance.

Tumor blood supply is normally through direct perfusion or/and vessel leakage. These vascular signatures impact radio-sensitivity by regulating the generation of oxygen free radical, which is involved in the repair of radiation-mediated DNA damage (4). Tumor vascular characteristics affect the degree of exposure to chemotherapy drugs, as well as drug activity levels *via* measuring the intra-tumor pH and the ratio of the quiescent cells in the tumor (5). As a non-invasive examining technique, MRI is widely applied worldwide and is already a standard staging protocol for cervical cancer. Dynamic contrast-enhanced magnetic resonance imaging (DCE-MRI) is regarded as a potential predictive option due to its capacity in the reflection of the perfusion by enhancement pattern, permeability, and the intratumoral angiogenic activity in the tumors (6, 7). DCE-MRI is thus applied to provide physiologic information of the tumor as well as anatomic details that are valuable for radiotherapy treatment response. These advantages make DCE-MRI an ideal tool in tumor perfusion studies that require repeated imaging.

DCE-MRI is widely applied as a non-invasive technique that plays an important role in predicting treatment response in various diseases (6, 8). Several studies have shown a correlation between DCE-MRI semiquantitative measurements and tumor response in cervical cancer patients (9). To date, there is a paucity of information in the literature about the predictive value of DCE-MRI quantitative parameters in treatment response for cervical cancer patients treated with CCRT.

The current standard treatment protocol for locally advanced cervical cancer patients is CCRT, regardless of the histological subtype of the disease. Several studies reported that patients with cervical adenocarcinoma had a poor response rate from treatment and overall survival than patients with squamous cell carcinoma (10, 11). To exclude the influence of histological subtype, we only enrolled squamous cell carcinoma patients.

This prospective study aimed to investigate the prognostic value of pre- and mid-treatment DCE-MRI quantitative parameters in the treatment prediction of patients with LACSC underwent CCRT.

METHODS AND MATERIALS

Patients

This single-center prospective study was approved by the Ethics Committee of Xijing Hospital and informed consent was obtained from all patients. From October 2018 to April 2019, 51 consecutive cervical cancer patients administered CCRT in the department of radiation oncology were prospectively recruited. The inclusion criteria were (1) histologic diagnosis of cervical squamous cell carcinoma, (2) planned to receive CCRT in our hospital, (3) the largest diameter of the cervical tumor was 1.0 cm or larger, and (4) no contraindications to DCE-MRI. All patients conducted DCE-MRI before and 3 days after CCRT. Three patients who changed treatment regimes were excluded. Thus, the final cohort analyzes 48 LACSC patients. Clinical characteristics are presented in **Table 1**.

Concurrent Chemoradiotherapy

All patients were treated with a combination of external beam radiotherapy (EBRT) and intracavitary brachytherapy (ICBT). EBRT was delivered to the whole pelvis with 15-MV photon beams at a daily dose of 2 Gy, 5 times per week, for a total dose of 50 Gy. EBRT was accompanied by concurrent chemotherapy: six cycles of weekly cisplatin (30 mg/mm²) in 30 patients and three cycles of 5-fluorouracil (1,000 mg/mm²) plus cisplatin (60 mg/mm²) at 3 weeks intervals in 18 patients. ICBT was delivered twice a week in 4 fractions with a fractional dose of 7 Gy at point A. the median overall treatment time was 59 days (range 45–71 days). The selection of the chemotherapeutic regime was individualized according to local tumor extent, pelvic lymph node involvement, and general patient condition (12).

Imaging Protocol

DCE-MRI was carried out at two time points: before the start of treatment (e0) and after 3 days of CCRT (e3). All MRI was performed at 3.0 T MRI system (Discovery MR 750, GE Medical Systems, Chicago, IL, USA) with an eight-channel phased-array Torso coil. The bladder was half-filled to improve lesion visibility. The scanning range covered the whole pelvis. Scanning parameters were as follows: axial fast spin-echo (FSE) T1-weighted images (T1WI) (repetition time[TR]/echo time

TABLE 1 | Baseline clinical characteristics of patients (n = 48).

Characteristics	Overall (n = 48)
Age (years), median (range)	55 (29–67)
FIGO stage, n (%)	
IB	2 (4.17%)
II	34 (70.83%)
III	8 (16.67%)
IVA	4 (8.33%)
Lymph node involvement, n (%)	
Negative	29 (60.42%)
Positive	19 (39.58%)
Overall treatment duration (days), Median (range)	59 (45–71)
The interval between pretreatment DCE-MRI and initial therapy (days), Median (range)	6 (2–9)

[TE]: 400 ms/7.3 ms, NEX: 2, slice thickness/gap: 5 mm/1 mm, field of view [FOV]: 380 × 380 mm, acquisition matrix: 384 × 256 mm); axial and sagittal fat suppression (FS) fast spin-echo (FSE) T2-weighted images (T2WI) (TR/TE: 4000 ms/130.2 ms, NEX: 2, slice thickness/gap: 5 mm/1 mm, FOV 380 × 224 mm, acquisition matrix: 240 × 240 mm).

DCE-MRI was performed using liver acquisition with volume acceleration-extended volume (LAVA-EV) sequence (TR/TE: 6.1 ms/1.1 ms, NEX: 1, slice thickness/gap: 4 mm/-2.0 mm, FOV: 260 × 260 mm; acquisition matrix: 256 × 128 mm) (TR/TE 3.6/1.8 ms, flip angle 3°, 6°, 9°, 12°, slice thickness 4 mm, no interslice gap, acquisition time 5 min 31 s). Before the injection of contrast material, unenhanced images were obtained by using axial 3D spoiled gradient recalled echo sequence series with flip angles of 3°, 6°, 9°, and 12°. Before and immediately after intravenous injection of 0.1 mmol/kg Gd-DTPA (Omniscan; GE Healthcare, Shanghai, China) at a rate of 3.0 ml/s, Dynamic images were obtained from the uterine fundus to the vulva and the total acquisition time was 320 s (8 s for each phase, 40 phases). Then, the delayed contrast-enhanced MR images for axial, coronal, and sagittal planes were obtained sequentially after dynamic contrast-enhanced MR images.

Image Analysis

Visible tumors were outlined by two radiologists on the sagittal T2WI and T1 dynamic images. Tumor volume was calculated by multiplying the area of tumor outlined on each T2WI by slice thickness. The final tumor regression rate (%) was calculated according to the following equation: $100 \times (\text{pretreatment volume} - \text{volume at 1 month after the finish of CCRT}) / \text{pretreatment volume}$. Previous studies have shown that the extent of the tumor regression rate correlates with survival (4).

Pharmacokinetic analysis was conducted using Omni-Kinetics (GE Healthcare, Life Science, Shanghai, China). User Arterial input function (AIF) was conducted by placing the ROI on the external iliac artery on the axial plane when reaching peak arterial enhancement (13, 14). The largest slice of the visible tumor on the axial plane was selected for arbitrarily ROI placement, which was carefully outlined around the tumor but avoiding cystic lesions with reference to T2WI, T1WI, and enhanced images. We used the Extended Tofts Linear model to generate endothelial transfer constant (K^{trans}), the reflux rate (K_{ep}), the fractional extravascular extracellular space (EES) volume (V_e), and the fractional plasma volume (V_p) (15). Based on the e0 and e3 DCE-MRI, the relative change in quantitative parameters were calculated, which were presented as Δ . Δ parameter (%) was calculated based on the following equation: $100 \times (\text{parameter-e3} - \text{parameter-e0}) / \text{parameter-e0}$.

Tumor Response Assessment

Response Evaluation Criteria in Solid Tumors (RECIST 1.1V) was used for treatment response assessment. Tumor response was assessed one month after the whole CCRT, which was conducted by treating doctors from the Department of radiation oncology. Patients with complete response were classified as non-residual tumor group, while patients with partial response, stable disease, and progressive disease were classified as residual tumor group.

Statistical Analysis

Quantitative parameters were presented as mean \pm standard deviation (SD). The zero values of K^{trans} were ruled out to exclude non-perfused/necrotic regions, where the pharmacokinetic model is not applicable.

Statistical analyses were performed using SPSS (Version 17.0, SPSS Inc., Chicago, IL, USA) and GraphPad Prism 8 (GraphPad Prism Software Inc., San Diego, California, USA). Spearman's correlation coefficient (r) was conducted to assess the correlation between quantitative parameters and tumor regression rate. Mann-Whitney U test was conducted to compare parameters between residual and non-residual tumor group. The predictive value of parameters was calculated by the receiver operating characteristic curve (ROC). Univariate and multivariate logistic regression analysis was conducted to find the independent variables. A two-tailed P value of less than 0.05 was considered statistically significant.

RESULTS

Patients

A total of 48 patients were eventually enrolled in this prospective study. Clinical characteristics for these patients are presented in **Table 1**. The median interval between pretreatment DCE-MRI and initial therapy was 6 days (range 2–9 days). The mean area from the ROIs was 11.2 cm² (ranged 2.3–35.8 cm²) in the pretreatment MRI scans and 4.3 cm² (range 0–8.4 cm²) in the 1 month after CCRT scans. The mean tumor volume before treatment was 45.64 cm³ (range 11.3–192.7 cm³) and 19.84 cm³ (range 0–92.84 cm³) at 1 month after CCRT. Mean tumor regression rate was 68.77% (ranged 41.77%–100%). One month after CCRT, 33 patients were categorized as non-residual tumor group and 15 patients were categorized as residual tumor group.

Quantitative Parameters in Non- and Residual Tumor Group Patients

The correlation between quantitative parameters and treatment outcome of LACSC to CCRT are presented in **Table 2**. The non-residual tumor group had higher pre- and mid-treatment K^{trans} and V_e changed more significantly compared with the residual tumor group. The delayed DCE-MRI and color maps are shown in **Figures 1 and 2**.

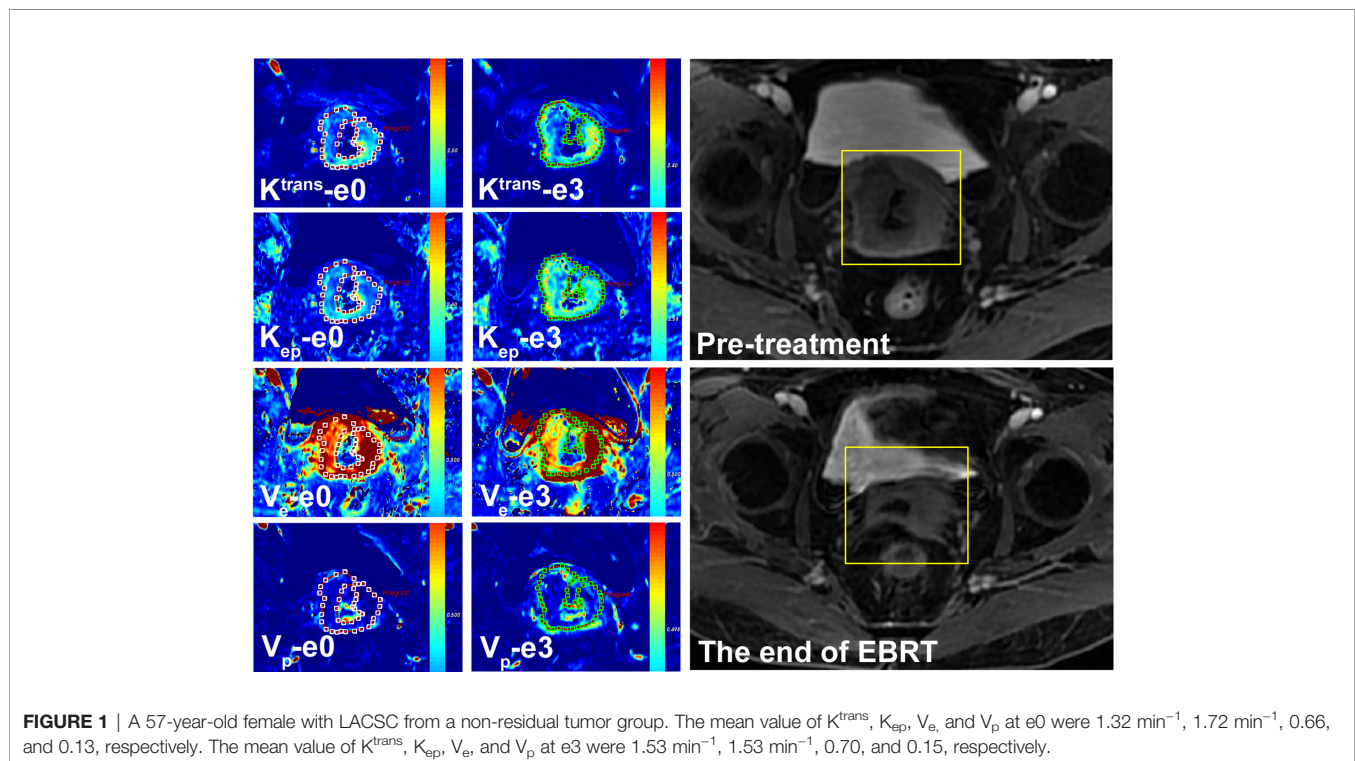
Tumor regression rate was positively correlated with $K^{\text{trans-e0}}$ ($r=0.576$, $P<0.001$), $K_{\text{ep-e0}}$ ($r = 0.528$, $P < 0.001$), $K^{\text{trans-e3}}$ ($r = 0.617$, $P = 0.025$), ΔK^{trans} ($r = 0.507$, $P < 0.001$) and ΔV_e ($r = 0.542$, $P < 0.001$). Details are presented in **Figure 3**.

The Receiver Operating Characteristic Curve, Univariate, and Multivariate Logistic Regression Analysis of Quantitative Parameters

The quantitative parameters exhibited good prognostic value to predict residual tumor occurrence, which was further validated by the ROC as presented in **Table 3** and **Figure 4**. $K^{\text{trans-e3}}$ showed the best predictive ability. When setting cut-off value of

TABLE 2 | Quantitative parameters and treatment response.

Quantitative parameters	Tumor regression rate (n = 48)		Non-residual tumor group (n = 33)	Residual tumor group (n = 15)	P value
	r value	P value			
$K^{trans}_{-e0}(\text{min}^{-1})$	0.576	<0.001*	1.36 ± 0.33	1.12 ± 0.35	0.04*
$K_{ep}_{-e0}(\text{min}^{-1})$	0.528	<0.001*	1.74 ± 0.39	1.67 ± 0.33	0.25
V_e_{-e0}	0.434	0.159	0.64 ± 0.22	0.64 ± 0.20	0.94
V_p_{-e0}	0.386	0.216	0.14 ± 0.08	0.13 ± 0.09	0.99
$K^{trans}_{-e3}(\text{min}^{-1})$	0.617	0.025*	1.58 ± 0.47	1.29 ± 0.46	0.02*
$K_{ep}_{-e3}(\text{min}^{-1})$	0.584	0.194	1.59 ± 0.43	1.53 ± 0.38	0.06
V_e_{-e3}	0.403	0.195	0.71 ± 0.17	0.63 ± 0.25	0.09
V_p_{-e3}	0.261	0.467	0.13 ± 0.11	0.15 ± 0.10	0.63
ΔK^{trans} (%)	0.507	<0.001*	41.54 ± 34.31	31.44 ± 33.15	0.04*
ΔK_{ep} (%)	0.410	0.186	-4.75 ± 30.36	-5.40 ± 28.67	0.75
ΔV_e (%)	0.542	<0.001*	25.80 ± 52.02	6.96 ± 46.94	0.01*
ΔV_p (%)	0.345	0.328	36.1 ± 64.32	57.75 ± 53.45	0.08

* $p < 0.05$.

K^{trans}_{-e3} to 1.48, the sensitivity, specificity, PPV and NPV were 81.82%, 80.00%, 81.82%, and 80.00%, with area under curve (AUC) of 0.753 ($P = 0.04$).

Univariate and multivariate logistic regression analysis revealed that K^{trans}_{-e0} , K^{trans}_{-e3} , and ΔV_e were independent prognostic factors for residual tumor occurrence. The lower K^{trans}_{-e0} , K^{trans}_{-e3} , ΔK^{trans} , and ΔV_e had higher risk ratios for residual tumor occurrence. Details are presented in **Table 4**.

DISCUSSION

CCRT is the primary option for the management of local advanced cervical cancer. Due to tumor heterogeneity, different

curative responses were found with the same treatment regimen. Early knowledge of treatment response is clinically significant and enables modification of treatment regimen in early the stage of applied treatment, which prevents unnecessary toxicity or prolonged ineffective consequence in treatment resisted patients.

In the present study, DCE-MRI was used to investigate the possibility to predict short-term response to CCRT and to improve diagnostic potency in cervical squamous cell carcinoma patients. Studies have shown that cervical squamous cell carcinoma had a better response rate from CCRT, took shorter time to achieve complete response, had better overall survival, and disease-free survival than adenocarcinoma (10, 16). Thus, we only enrolled patients with cervical squamous cell carcinoma, to exclude the influence by histology type.

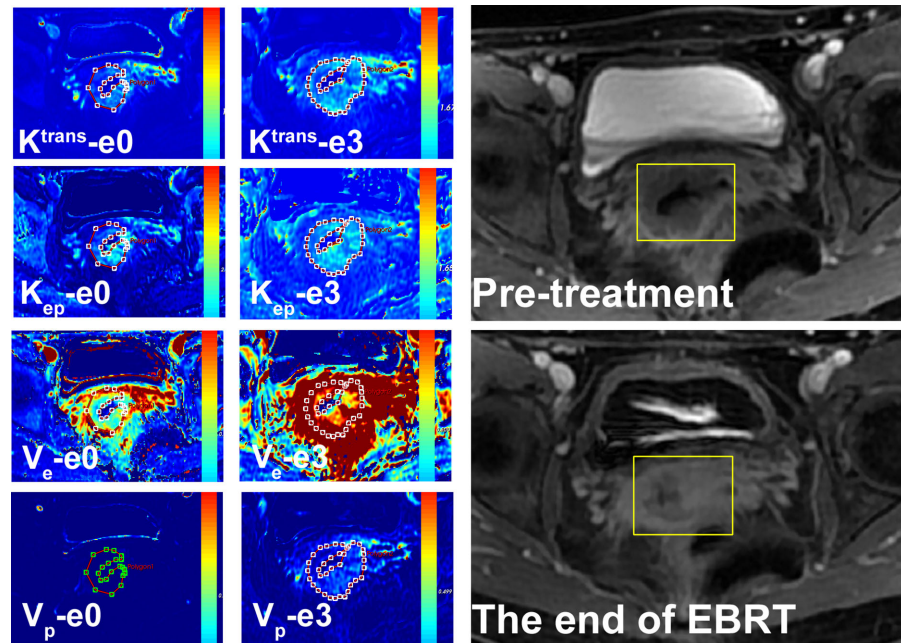


FIGURE 2 | A 54-year-old female with LACSC from residual tumor group. The mean value of K^{trans} , K_{ep} , V_e , and V_p at e0 were 1.11 min^{-1} , 1.68 min^{-1} , 0.63 , and 0.14 , respectively. The mean value of K^{trans} , K_{ep} , V_e , and V_p at e3 were 1.32 min^{-1} , 1.56 min^{-1} , 0.65 , and 0.14 , respectively.

Tumor regression rate was chosen as a short-term endpoint due to its close relationship with local control and outcome of cancer management (17, 18). Here, we found that quantitative DCE-MRI parameters $K^{\text{trans-e0}}$, $K_{\text{ep-e0}}$, $K^{\text{trans-e3}}$, ΔK^{trans} , and ΔV_e positively correlated with tumor regression rate in LACSC. Accumulating evidence has shown the correlation between DCE-MRI parameters and tumor regression. Several studies concluded that pretreatment parameters K^{trans} and K_{ep} were positively correlated with tumor regression rate (4, 19, 20), which is inconsistent with our results. However, Park et al. reported that pretreatment K^{trans} positively correlated with tumor volume at 4 weeks of initiating CCRT (21). To our knowledge, K^{trans} and K_{ep} reflect the permeability of tumor tissue, this property has a positive influence on oxygenation within tumor tissue, which results in higher radiation sensitivity. What's more, hypoxia is a known cause of clinical radioresistance for cervical cancer (22). Therefore, tumors with higher permeability tend to respond to better treatment outcomes and thus lead to higher tumor regression rate.

Additionally, our results revealed that mid-treatment $K^{\text{trans-e3}}$, and the increase of K^{trans} positively correlated with tumor regression rate as well. The non-residual tumor group showed higher K^{trans} at e3, together with ΔK^{trans} . Mid treatment K^{trans} value represents early treatment response to CCRT, which could be interpreted as K^{trans} reflect the effectiveness of oxygen and chemotherapy drugs between plasma and interstitial space of the tumor. Higher mid-treatment K^{trans} value can be explained as increasing levels of permeability due to the disintegration of tumor cell and capillary membranes, which are a consequence of chemoradiotherapy.

V_e reflects the extravascular extracellular space, and lower V_e value could be interpreted as higher cellularity (23). The increase of V_e may reflect the enlargement of fractional EES, which indicates the decrease in cell density. Several studies concerning V_e and its correlation with treatment response showed different results. Ellingsen et al. reported that pretreatment V_e showed no association with hypoxia in cervical cancer xenografts (24). Kim et al. showed that the early increase of V_e was associated with tumor regression in cervical cancer patients underwent CCRT (25). Also, Cheng et al. reported similar results in lung carcinoma that an early increase in V_e is correlated with tumor control (26). The above studies supported our results. However, Park et al. reported that pretreatment V_e negatively correlated with tumor volume at 1 month after the end of treatment (21). Their results suggested that higher pretreatment K^{trans} and lower pretreatment V_e tended to result in a larger tumor volume at 4 weeks of CCRT. They argued this was caused by secondary inflammation related to ongoing treatment. We hold the opinion that V_e represents a direct estimation of EES to which a contrast agent or drug can be delivered. The increase of V_e was the result of a decrease of tumor cell density and enlargement of the distribution space, which enables more contrast agent and chemotherapy drugs to be delivered, leading to a higher tumor regression rate.

DCE-MRI parameters have been extensively used in predicting tumor response to radiotherapy and chemotherapy (27), to non-invasively investigate tumor microvascular structure and heterogeneity, thus providing additional information to potentially improve sensitivity to the treatment regimen. We incorporated two time-points to investigate if DCE-MRI

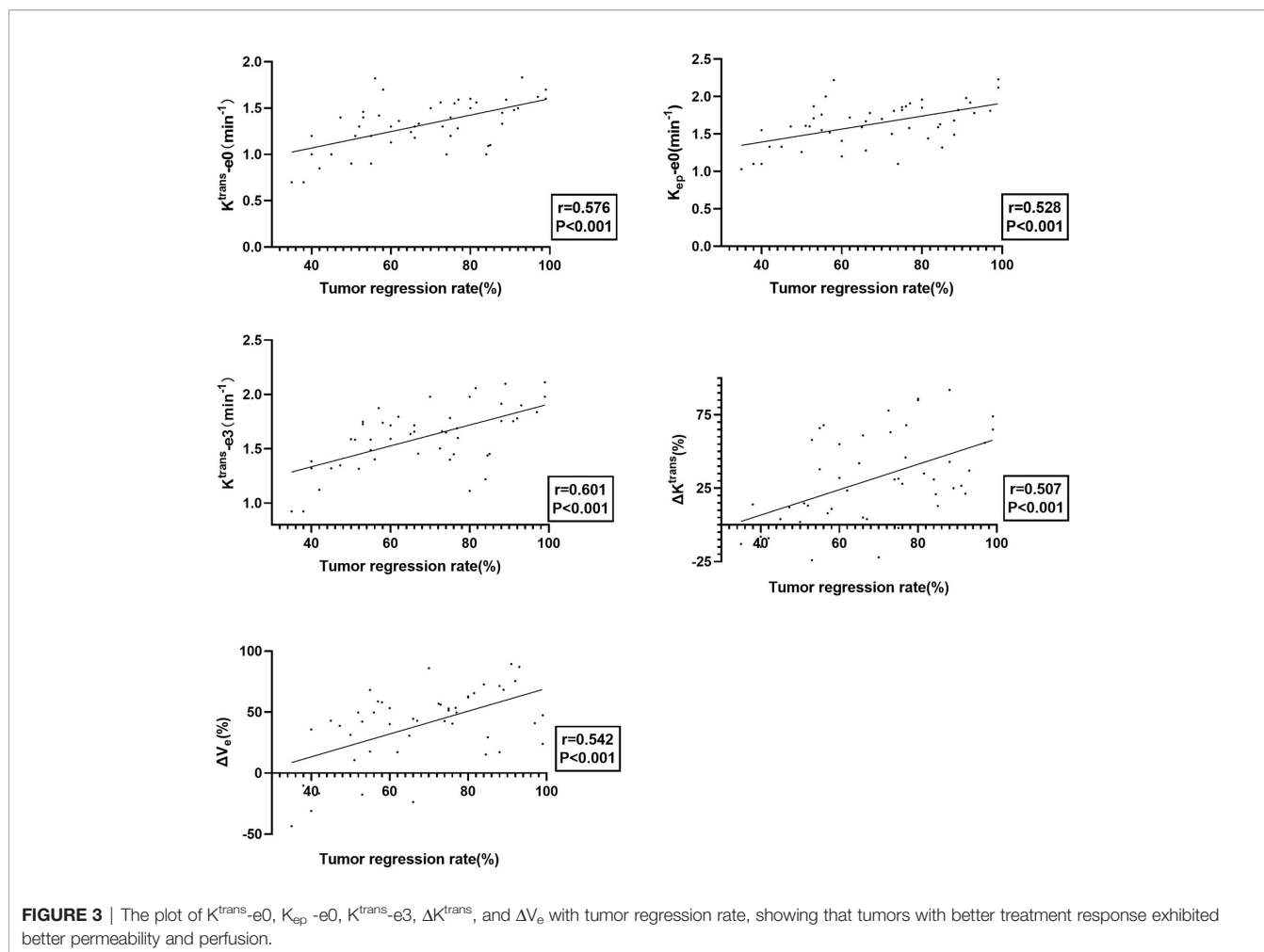


TABLE 3 | Values of quantitative parameters for predicting residual tumor occurrence.

	AUC	Cut-off	Sensitivity(%)	Specificity(%)	PPV(%)	NPV(%)	P value
$K^{\text{trans}}\text{-e0}$ (min^{-1})	0.750	1.21	87.50	72.50	92.11	50.00	0.03*
$K^{\text{trans}}\text{-e3}$ (min^{-1})	0.753	1.48	81.82	80.00	81.82	80.00	0.04*
ΔK^{trans} (%)	0.734	45.57	72.22	70.43	79.63	71.48	0.04*
ΔV_e (%)	0.711	36.4	77.78	66.67	82.35	60.00	0.02*

AUC, area under the curve; PPV, positive predictive value; NPV, negative predictive value; * $p < 0.05$.

quantitative parameters can predict treatment response, and revealed that $K^{\text{trans}}\text{-e0}$, $K^{\text{trans}}\text{-e3}$, ΔK^{trans} , and ΔV_e could be biomarkers to predict treatment response for LACSC. Several studies are partially consistent with our results. Tao et al. reported that pretreatment K^{trans} and K_{ep} were significantly higher and V_e were lower in responders than the non-responder group in non-small cell lung cancer (19). Kim et al. found in breast cancer pretreatment DCE-MRI parameters showed no difference, while after two cycles of NACT, the change of K^{trans} and K_{ep} were significantly higher in good responder group (28). Wong et al. reported in advanced head and neck cancer that larger fractional increase in K^{trans} and V_e in responders versus non-responders at week 2 of treatment (29). Several studies are showing conflicting results. Andersen et al. reported that pretreatment K^{trans} and V_e

were positively correlated with progression-free survival for cervical cancer patients (30). Zheng et al. reported that K^{trans} was higher and V_e was lower in non-residual group cervical cancer patients (31). Semple et al. proved that pretreatment K^{trans} correlated with the response in cervical cancer patients (32). We found that $K^{\text{trans}}\text{-e0}$, $K^{\text{trans}}\text{-e3}$, ΔK^{trans} , and ΔV_e are significantly higher in the non-residual tumor group than the residual tumor group in LACSC. The parameters $K^{\text{trans}}\text{-e0}$, $K^{\text{trans}}\text{-e3}$, and ΔK^{trans} were significantly higher in non-residual tumor group patients, which supported the hypothesis that better permeability represented better material exchange, thus better oxygenation and higher radiation sensitivity (33). Low oxygen level within tumor tissue, i.e., hypoxia causes therapeutic resistance *via* reducing the generation of oxygen free radical, which interferes with the repair of DNA damage induced by

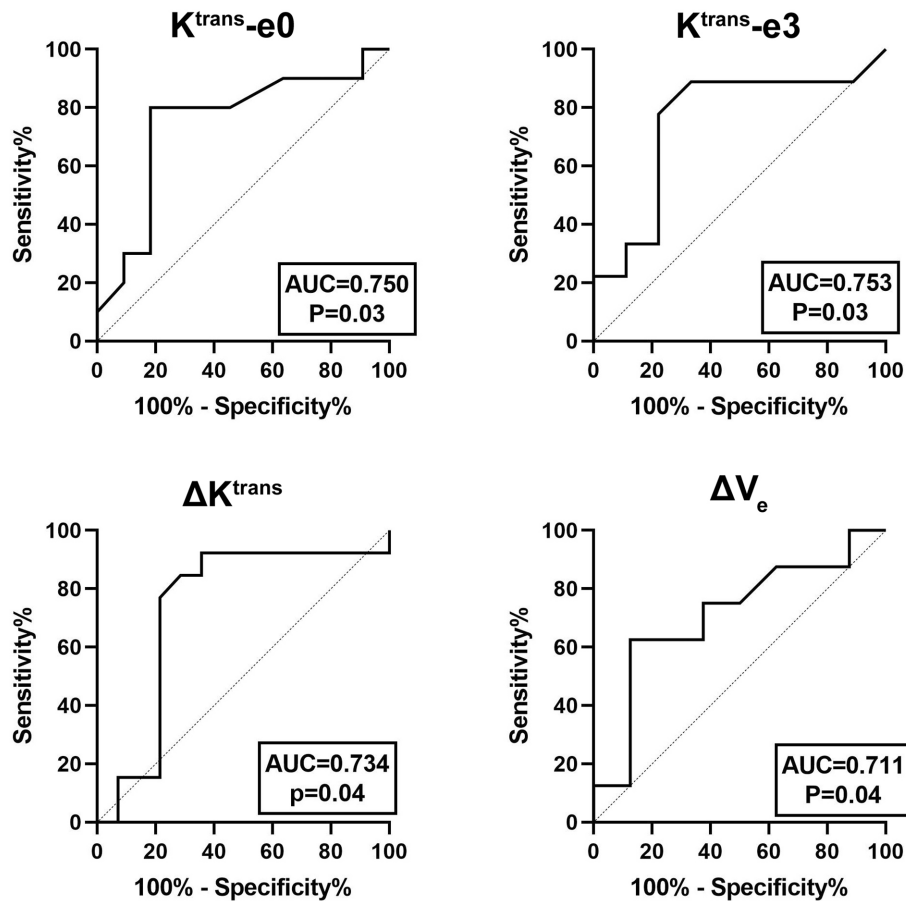


FIGURE 4 | ROC curves for predicting residual tumor occurrence based on $K^{\text{trans}}_{\text{-e0}}$, $K^{\text{trans}}_{\text{-e3}}$, ΔK^{trans} , and ΔV_e . The area under curve (AUC) was 0.750, 0.753, 0.734, and 0.711, respectively.

TABLE 4 | Univariate and multivariate logistic regression analysis for predicting residual tumor occurrence.

Parameters	OR	P value	95% CI
Univariate analysis			
$K^{\text{trans}}_{\text{-e0}}$ (min^{-1})	15.6	0.03*	1.53–104.13
$K^{\text{trans}}_{\text{-e3}}$ (min^{-1})	25.4	<0.01*	5.74–78.31
ΔK^{trans} (%)	7.9	0.02*	1.36–34.52
ΔV_e (%)	6.5	0.03*	1.07–29.84
Multivariate analysis			
$K^{\text{trans}}_{\text{-e0}}$ (min^{-1})	18.00	<0.01*	1.74–114.40
$K^{\text{trans}}_{\text{-e3}}$ (min^{-1})	21.00	<0.01*	4.89–68.42
ΔK^{trans} (%)	5.1	0.01*	2.34–11.72
ΔV_e (%)	7.00	0.04*	1.11–32.30

OR, odds ratio; CI, confidence interval; * $p < 0.05$.

radiotherapy, thus transferring tumor cells into subtypes with more resistance to treatment regimens (34, 35). The non-residual tumor group showed higher permeability before and early during treatment, resulting in higher radio-sensitivity and access to chemotherapeutic drugs. Tumors with a higher level of perfusion and permeability are likely to be better oxygenated and therefore more sensitive to radiation. Moreover, higher perfusion also results

in a higher concentration of chemotherapy drugs within the tumor. Evidence showed that low V_e was negatively correlated with progression-free survival, indicating that patients with high cell density had a more aggressive disease, which also supported our results.

Finally, we showed that day 3 of CCRT could be a time point to detect treatment response using DCE-MRI quantitative parameters. To our knowledge, this is the first study investigating the complementary value of DCE-MRI quantitative parameters on the 3rd day of CCRT for response prediction in patients with LACSC. Previous studies applied the time point of week 1, week 2, or week 4 (34, 35). Early detection of treatment response is important since it can avoid unnecessary toxicity and treatment-related complications. Early prediction of response during treatment may enable early modification of treatment (i.e., radiation dosage intensification or discontinuation) (28). We noticed that AUC of mid-treatment $K^{\text{trans}}_{\text{-e3}}$ was higher than pretreatment $K^{\text{trans}}_{\text{-e0}}$, probably indicated that the closer relation between mid-treatment parameter and treatment outcome.

There are several limitations in this single-center retrospective study. Firstly, the follow-up period was short, and overall survival or progression-free survival were not analyzed.

Thus, we did not evaluate the correlation between pre- or mid-therapy DCE-MRI parameters and those clinical endpoints. Secondly, more time points should be set to get a full view of the dynamic change of quantitative parameters during the whole treatment process. Thirdly, further investigation should be done to investigate the correlation between oxygenation and treatment response.

In conclusion, our preliminary results showed that quantitative parameters at e_0 and e_3 from DCE-MRI could be used as a potential indicator for predicting treatment response of LACSC. The mean value of $K^{trans-e_0}$, $K^{trans-e_3}$, ΔK^{trans} , and ΔV_e is potentially applicable for treatment response prediction. $K^{trans-e_0}$, K_{ep-e_0} , ΔK^{trans} , and ΔV_e can be used for predicting tumor regression rate. Further studies are needed to clarify the possibility to detect heterogeneity directly by MRI techniques. Our study therefore strongly suggests that DCE-MRI may be a useful tool for individualizing therapy of LACSC.

DATA AVAILABILITY STATEMENT

All datasets presented in this study are included in the article/supplementary material.

REFERENCES

- Bray F, Ferlay J, Siegel RL, Torre LA, Jemal A. Global cancer statistics 2018: GLOBOCAN estimates of incidence and mortality worldwide for 36 cancers in 185 countries. *CA Cancer J Clin* (2018) 68(6):394–424. doi: 10.3322/caac.21492
- Green JA, Kirwan JM, Tierney JF, Symonds P, Fresco L, Collingwood M, et al. Survival and recurrence after concomitant chemotherapy and radiotherapy for cancer of the uterine cervix: a systematic review and meta-analysis. *Lancet* (2001) 358(9284):781–6. doi: 10.1016/S0140-6736(01)05965-7
- Overgaard J, Hansen HS, Overgaard M, Bastholt L, Berthelsen A, Specht L, et al. A randomized double-blind phase III study of nimorazole as a hypoxic radiosensitizer of primary radiotherapy in supraglottic larynx and pharynx carcinoma. Results of the Danish Head and Neck Cancer Study (DAHANCA) Protocol 5-85. *Radiother Oncol* (1998) 46(2):135–46. doi: 10.1016/S0167-8140(97)00220-X
- Zahra MA, Tan LT, Priest AN, Graves MJ, Arends M, Crawford RAF, et al. Semiquantitative and Quantitative Dynamic Contrast-Enhanced Magnetic Resonance Imaging Measurements Predict Radiation Response in Cervix Cancer. *Int J Radiat Oncol Biol Physics* (2009) 74(3):766–73. doi: 10.1016/j.ijrobp.2008.08.023
- Jensen RL, Mumert ML, Gillespie DL, Kinney AY, Schabel MC, Salzman KL, et al. Preoperative dynamic contrast-enhanced MRI correlates with molecular markers of hypoxia and vascularity in specific areas of intratumoral microenvironment and is predictive of patient outcome. *Neuro Oncol* (2014) 16(2):280–91. doi: 10.1093/neuonc/not148
- Zahra MA, Hollingsworth KG, Sala E, Lomas DJ, Tan LT. Dynamic contrast-enhanced MRI as a predictor of tumour response to radiotherapy. *Lancet Oncol* (2007) 8(1):63–74. doi: 10.1016/S1470-2045(06)71012-9
- Hawighorst H, Knapstein PG, Knopp MV, Weikel W, Brix G, Zuna I, et al. Uterine cervical carcinoma: comparison of standard and pharmacokinetic analysis of time-intensity curves for assessment of tumor angiogenesis and patient survival. *Cancer Res* (1998) 58(16):3598–602.
- Li SP, Padhani AR. Tumor response assessments with diffusion and perfusion MRI. *J Magn Reson Imaging* (2012) 35(4):745–63. doi: 10.1002/jmri.22838
- Yang W, Qiang JW, Tian HP, Chen B, Wang AJ, Zhao JG. Multi-parametric MRI in cervical cancer: early prediction of response to concurrent chemoradiotherapy in combination with clinical prognostic factors. *Eur Radiol* (2018) 28(1):437–45. doi: 10.1007/s00330-017-4989-3
- Katanyoo K, Sanguanrungrasirikul S, Manusirivithaya S. Comparison of treatment outcomes between squamous cell carcinoma and adenocarcinoma in locally advanced cervical cancer. *Gynecol Oncol* (2012) 125(2):292–6. doi: 10.1016/j.ygyno.2012.01.034
- Feng Y, Liu H, Ding Y, Zhang Y, Liao C, Jin Y, et al. Combined dynamic DCE-MRI and diffusion-weighted imaging to evaluate the effect of neoadjuvant chemotherapy in cervical cancer. *Tumori* (2020) 106(2):155–64. doi: 10.1177/0300891619886656
- Liu B, Ma WL, Zhang GW, Sun Z, Zhong JM, Wei MQ, et al. Changes in magnetic resonance T2-weighted imaging signal intensity correlate with concurrent chemoradiotherapy response in cervical cancer. *J Contemp Brachyther* (2019) 11(1):41–7. doi: 10.5114/jcb.2019.83285
- Chen J, Yao J, Thomasson D. Automatic determination of arterial input function for dynamic contrast enhanced MRI in tumor assessment. *Med Image Comput Comput Assist Interv* (2008) 11:594–601. doi: 10.1007/978-3-540-85988-8_71
- Huang W, Chen Y, Li X, Jajamovich GH, Malyarenko DI, Aryal MP, et al. The Impact of Arterial Input Function Determination Variations on Prostate Dynamic Contrast-Enhanced Magnetic Resonance Imaging Pharmacokinetic Modeling: A Multicenter Data Analysis Challenge. *Tomography* (2016) 2(1):56–66. doi: 10.18383/j.tom.2015.00184
- Tofts PS. Modeling tracer kinetics in dynamic Gd-DTPA MR imaging. *J Magn Reson Imaging* (1997) 7(1):91–101. doi: 10.1002/jmri.1880070113
- Hu K, Wang W, Liu X, Meng Q, Zhang F. Comparison of treatment outcomes between squamous cell carcinoma and adenocarcinoma of cervix after definitive radiotherapy or concurrent chemoradiotherapy. *Radiat Oncol* (2018) 13(1):249. doi: 10.1186/s13014-018-1197-5
- Hardt N, van Nagell JR, Hanson M, Donaldson E, Yoneda J, Maruyama Y, et al. Radiation-induced tumor regression as a prognostic factor in patients with invasive cervical cancer. *Cancer-Am Cancer Soc* (1982) 49(1):35–9. doi: 10.1002/1097-0142(19820101)49:1<35::AID-CNCR2820490108>3.0.CO;2-3
- Hong JH, Chen MS, Lin FJ, Tang SG. Prognostic assessment of tumor regression after external irradiation for cervical cancer. *Int J Radiat Oncol Biol Phys* (1992) 22(5):913–7. doi: 10.1016/0360-3016(92)90787-I

ETHICS STATEMENT

The studies involving human participants were reviewed and approved by Ethics Committee of Xijing Hospital. The patients/participants provided their written informed consent to participate in this study. Written informed consent was obtained from the individual(s) for the publication of any potentially identifiable images or data included in this article.

AUTHOR CONTRIBUTIONS

YH and M-WZ conceived and designed this study. JR, M-LM, and W-HH conducted the study. B-XH and L-CW collected important background data. BL and ZS drafted the manuscript. All authors contributed to the article and approved the submitted version.

FUNDING

This work was supported by Chinese National Natural Science Foundation Grants (No. 81220108011).

19. Tao X, Wang L, Hui Z, Liu L, Ye F, Song Y, et al. DCE-MRI Perfusion and Permeability Parameters as predictors of tumor response to CCRT in Patients with locally advanced NSCLC. *Sci Rep* (2016) 6:35569. doi: 10.1038/srep35569
20. Yamashita Y, Baba T, Baba Y, Nishimura R, Ikeda S, Takahashi M, et al. Dynamic contrast-enhanced MR imaging of uterine cervical cancer: pharmacokinetic analysis with histopathologic correlation and its importance in predicting the outcome of radiation therapy. *Radiology* (2000) 216(3):803–9. doi: 10.1148/radiology.216.3.r00se07803
21. Park JJ, Kim CK, Park SY, Simonetti AW, Kim E, Park BK, et al. Assessment of early response to concurrent chemoradiotherapy in cervical cancer: value of diffusion-weighted and dynamic contrast-enhanced MR imaging. *Magn Reson Imaging* (2014) 32(8):993–1000. doi: 10.1016/j.mri.2014.05.009
22. Vaupel P, Mayer A. Hypoxia in cancer: significance and impact on clinical outcome. *Cancer Metastasis Rev* (2007) 26(2):225–39. doi: 10.1007/s10555-007-9055-1
23. Egeland TA, Gaustad JV, Galappathi K, Rofstad EK. Magnetic resonance imaging of tumor necrosis. *Acta Oncol* (2011) 50(3):427–34. doi: 10.3109/0284186X.2010.526633
24. Ellingsen C, Hompland T, Galappathi K, Mathiesen B, Rofstad EK, et al. DCE-MRI of the hypoxic fraction, radioresponsiveness, and metastatic propensity of cervical carcinoma xenografts. *Radiother Oncol* (2014) 110(2):335–41. doi: 10.1016/j.radonc.2013.10.018
25. Kim JH, Kim CK, Park BK, Park SY, Huh SJ, Kim B. Dynamic contrast-enhanced 3-T MR imaging in cervical cancer before and after concurrent chemoradiotherapy. *Eur Radiol* (2012) 22(11):2533–9. doi: 10.1007/s00330-012-2504-4
26. Cheng JC, Yuan A, Chen JH, Lu YC, Cho KH, Wu JK, et al. Early detection of Lewis lung carcinoma tumor control by irradiation using diffusion-weighted and dynamic contrast-enhanced MRI. *PLoS One* (2013) 8(5):e62762. doi: 10.1371/journal.pone.0062762
27. Heethuis SE, Goense L, van Rossum P, Borggreve AS, Mook S, Voncken F, et al. DW-MRI and DCE-MRI are of complementary value in predicting pathologic response to neoadjuvant chemoradiotherapy for esophageal cancer. *Acta Oncol* (2018) 57(9):1201–8. doi: 10.1080/0284186X.2018.1473637
28. Kim Y, Kim SH, Song BJ, Kang BJ, Yim KI, Lee A, et al. Early Prediction of Response to Neoadjuvant Chemotherapy Using Dynamic Contrast-Enhanced MRI and Ultrasound in Breast Cancer. *Korean J Radiol* (2018) 19(4):682–91. doi: 10.3348/kjr.2018.19.4.682
29. Wong KH, Panek R, Dunlop A, McQuaid D, Riddell A, Welsh LC, et al. Changes in multimodality functional imaging parameters early during chemoradiation predict treatment response in patients with locally advanced head and neck cancer. *Eur J Nucl Med Mol Imaging* (2018) 45(5):759–67. doi: 10.1007/s00259-017-3890-2
30. Andersen EK, Hole KH, Lund KV, Sundfor K, Kristensen GB, Lyng H, et al. Pharmacokinetic parameters derived from dynamic contrast enhanced MRI of cervical cancers predict chemoradiotherapy outcome. *Radiother Oncol* (2013) 107(1):117–22. doi: 10.1016/j.radonc.2012.11.007
31. Zheng X, Guo W, Dong J, Qian L. Prediction of early response to concurrent chemoradiotherapy in cervical cancer: Value of multi-parameter MRI combined with clinical prognostic factors. *Magn Reson Imaging* (2020). doi: 10.1016/j.mri.2020.06.014
32. Semple SII, Harry VN, Parkin DE, Gilbert FJ. A combined pharmacokinetic and radiologic assessment of dynamic contrast-enhanced magnetic resonance imaging predicts response to chemoradiation in locally advanced cervical cancer. *Int J Radiat Oncol Biol Phys* (2009) 75(2):611–7. doi: 10.1016/j.ijrobp.2009.04.069
33. Cho H, Ackerstaff E, Carlin S, Lupu ME, Wang Y, Rizwan A, et al. Noninvasive multimodality imaging of the tumor microenvironment: registered dynamic magnetic resonance imaging and positron emission tomography studies of a preclinical tumor model of tumor hypoxia. *Neoplasia* (2009) 11(3):247–59, 2p-259p. doi: 10.1593/neo.81360
34. Mayer A, Vaupel P. Hypoxia, lactate accumulation, and acidosis: siblings or accomplices driving tumor progression and resistance to therapy? *Adv Exp Med Biol* (2013) 789:203–9. doi: 10.1007/978-1-4614-7411-1_28
35. Halle C, Andersen E, Lando M, Aarnes EK, Hasvold G, Holden M, et al. Hypoxia-induced gene expression in chemoradioresistant cervical cancer revealed by dynamic contrast-enhanced MRI. *Cancer Res* (2012) 72(20):5285–95. doi: 10.1158/0008-5472.CAN-12-1085

Conflict of Interest: The authors declare that the research was conducted in the absence of any commercial or financial relationships that could be construed as a potential conflict of interest.

Copyright © 2020 Liu, Sun, Ma, Ren, Zhang, Wei, Hou, Hou, Wei, Huan and Zheng. This is an open-access article distributed under the terms of the Creative Commons Attribution License (CC BY). The use, distribution or reproduction in other forums is permitted, provided the original author(s) and the copyright owner(s) are credited and that the original publication in this journal is cited, in accordance with accepted academic practice. No use, distribution or reproduction is permitted which does not comply with these terms.